

Supplementing State and Dynamics Estimation with Information from Optimal Control Policies

Daniel P. Lubey¹ and Daniel J. Scheeres²

Abstract—In this paper, we address dynamically mismodeled systems, and how those mismodeled dynamics may be detected and recovered. We combine an optimal control process with an optimal estimator to yield an algorithm that outputs simultaneous state and control estimates. This new estimator (the Optimal Control Based Estimator) is shown to be a generalization of the Kalman filter with automatic dynamic noise propagation and smoothing properties. The control estimates it outputs contain information about the mismodeled dynamics. Complimentary algorithms that detect and reconstruct maneuvers from the information in the control policies are developed. A simulation in which these algorithms are applied to an astrodynamics tracking problem shows how this algorithm may be used to estimate a system's state, detect mismodeled dynamics, and reconstruct those dynamics.

I. INTRODUCTION

Understanding the natural dynamics and control capabilities of objects in Earth orbit is essential to ensuring the safety and accessibility of this environment due to the growing risk of collision that follows from the increasing population density. In understanding natural dynamics we can more easily locate the objects at a given time, improve estimation capability, and make long term propagations more accurate - all of which are necessary for accurate collision prediction. While gravitational perturbations are well-studied and universal, object dependent perturbations like atmospheric drag and solar radiation pressure require direct knowledge of the object's physical parameters that are not readily accessible. Similarly, the control capabilities of active spacecraft are not readily available given the international and industry nature of the aerospace community, but this information is still desired to properly understand the dynamics and evolution of the overall system. As such, we desire methods that allow us to extract dynamical information about objects in orbit through independent observation.

Beyond desiring an algorithm that only requires independent (non-cooperative) observation, we also require this method to be implementable into a data-sparse environment. By its very nature, astrodynamics and Space Situational Awareness (SSA) are data-sparse fields, meaning observations (often with large uncertainty and indirect state relations) are taken at much smaller rates compared to the quick dynamics of the system. Methods such as Bar-Shalom and Birmiwal's Variable Dimension Filter [1] and Chan, Hu,

and Plant's Input Estimation Method [2] directly append accelerations to the state vector for estimation when a maneuver is detected through residuals, but such methods require observation throughout a continuous maneuver. In this context we define maneuver as any unknown (unmodeled / mismodeled) acceleration whether its natural or controlled. Patera's space event detection method [3] focuses more on quick events in an astrodynamics context, so it tends to neglect smaller maneuvers and natural dynamics mismodeling. Holzinger, Scheeres, and Alfriend [4] addressed the problems of object correlation, maneuver detection, and maneuver characterization for data sparse environments by implementing a Control Distance Metric based on a quadratic control policy. Singh, Horwood, and Poore [5] adapted the Control Distance Metric approach by using a minimum-fuel cost function. Lubey and Scheeres used this framework and adapted it into a filter formulation ([6], [7], [8], [9]) that yields state and control estimates. The authors also explored how these control estimates may be analyzed in an astrodynamics focused algorithm that estimates atmospheric drag and Solar Radiation Pressure (SRP) from control profiles [10]. This paper combines the filter and control analysis algorithms together into a filter formulation capable of state estimation, control estimation, maneuver detection, maneuver reconstruction, and natural dynamics estimation in data sparse systems with independent observation. We focus on generalizing the algorithm for application in any system.

This study summarizes this new estimator and how its control estimates may be used for maneuver detection and reconstruction. Section II gives a brief overview of optimal control since it lies at the heart of this estimator. Section III outlines how the filter is derived and its properties. Section IV highlights how the control estimates may be used for maneuver detection and reconstruction. Section V presents a simulation in which the filter is implemented in an astrodynamics tracking problem with mismodeled dynamics. Finally, onclusions are given in Section VI.

II. GENERATING OPTIMAL CONTROL POLICIES

The process of deriving an Optimal Control Policy using a generic cost function is summarized below, as it plays a crucial role in our filter and the control policy analysis. More detailed accounts are provided by Lawden [11], [12], Marec [13], Stengel [14], and Prussing [15], [16] among others.

An arbitrary cost function may be written in the Bolza form shown in Eqn. 1. In this notation the Lagrangian portion of the cost (\mathcal{L}) is evaluated across the entire time of flight, whereas the boundary costs (K_0 and K_f) are evaluated only

¹Daniel P. Lubey is a graduate research assistant in the department of Aerospace Engineering Sciences, University of Colorado at Boulder, CO 80309 daniel.lubey@colorado.edu

²Daniel J. Scheeres is the A. Richard Seebass Chair Professor in the Department of Aerospace Engineering Sciences, University of Colorado at Boulder, CO 80309 scheeres@colorado.edu

at the initial and/or final epochs. In this notation \bar{x} refers to the state of the system, \bar{u} refers to control inputs into the system, and the subscripts indicate at what epoch the values are evaluated (0 = initial epoch and f = final epoch). To fully define the system, we make the following definitions: $\bar{x} \in \mathbb{R}^n$; $\bar{u} \in \mathbb{R}^m$; and K_0 , K_f , and \mathcal{L} are scalar functions .

$$\mathcal{J} = K_0(\bar{x}_0, t_0) + K_f(\bar{x}_f, t_f) + \int_{t_0}^{t_f} \mathcal{L}(\bar{x}(\tau), \bar{u}(\tau), \tau) d\tau \quad (1)$$

In addition to these soft constraints, hard constraints are imposed via Lagrange multipliers ($\bar{\mu}_0, \bar{\mu}_f$, and $\bar{p}(t)$). The first two hard constraints force the initial and final times and states to lie on given manifolds ($\{g_0(\bar{x}_0, t_0) = \bar{0}\} \in \mathbb{R}^q$ and $\{g_f(\bar{x}_f, t_f) = \bar{0}\} \in \mathbb{R}^s$). The final hard constraint enforces the state dynamics to adhere to a given function of the state, control, and time ($\dot{\bar{x}}(t) = \bar{f}(\bar{x}(t), \bar{u}(t), t)$). The Lagrange multiplier that enforces this constraint ($\bar{p}(t) \in \mathbb{R}^n$) is termed the system's adjoint or costate. The adjointed cost function is provided in Eqn. 2.

$$\begin{aligned} \mathcal{J}_A = & \left[K_0(\bar{x}_0, t_0) + \bar{\mu}_0^T g_0(\bar{x}_0, t_0) \right] \\ & + \left[K_f(\bar{x}_f, t_f) + \bar{\mu}_f^T g_f(\bar{x}_f, t_f) \right] \\ & + \int_{t_0}^{t_f} \left[\mathcal{L}(\bar{x}(\tau), \bar{u}(\tau), \tau) \right. \\ & \left. + \bar{p}(\tau)^T (\bar{f}(\bar{x}(\tau), \bar{u}(\tau), \tau) - \dot{\bar{x}}(\tau)) \right] d\tau \end{aligned} \quad (2)$$

Freeing up the boundary times and states when taking the first variation of the cost we obtain the necessary conditions for optimality given in Eqns. 4-10 subject to the definition made in Eqn. 3. As shown in this definition, the optimally controlled system may be defined using a Hamiltonian formulation. This provides useful properties (such as the symplectic state transition matrix), which may be used in analytical manipulation. The first necessary condition (Eqn. 4) defines the optimal control policy ($\bar{u}(t)$) in terms of the state and adjoint using the result from the Pontryagin Minimum Principle. The next two necessary conditions (Eqns. 5 and 6) provide equations of motion for the state and adjoint, respectively. The final four necessary conditions (Eqns. 7 - 10) are the transversality conditions, which set boundary conditions on the initial and final times and adjoints. In these equations \mathcal{H}_0 and \mathcal{H}_f represent the Hamiltonian evaluated the initial and final epoch, respectively.

$$\mathcal{H}(\bar{x}(t), \bar{u}(t), \bar{p}(t), t) = \mathcal{L}(\bar{x}(t), \bar{u}(t), t) + \bar{p}(t)^T \bar{f}(\bar{x}(t), \bar{u}(t), t) \quad (3)$$

$$\bar{u}(t) = \underset{\bar{u}}{\operatorname{argmin}} (\mathcal{H}(\bar{x}(t), \bar{u}(t), \bar{p}(t), t)) \quad (4)$$

$$\dot{\bar{x}}(t) = \frac{\partial \mathcal{H}}{\partial \bar{p}} = \bar{f}(\bar{x}(t), \bar{u}(t), t) \quad (5)$$

$$\dot{\bar{p}}(t) = -\frac{\partial \mathcal{H}}{\partial \bar{x}} = -\frac{\partial \mathcal{L}}{\partial \bar{x}} - \frac{\partial \bar{f}^T}{\partial \bar{x}} \bar{p}(t) \quad (6)$$

$$\mathcal{H}_0 = \frac{\partial K_0(\bar{x}(t_0), t_0)}{\partial t} + \bar{\mu}_0^T \frac{\partial g_0(\bar{x}(t_0), t_0)}{\partial t} \quad (7)$$

$$\bar{p}(t_0) = -\frac{\partial K_0(\bar{x}(t_0), t_0)}{\partial \bar{x}} - \frac{\partial g_0(\bar{x}(t_0), t_0)}{\partial \bar{x}} \bar{\mu}_0 \quad (8)$$

$$\mathcal{H}_f = -\frac{\partial K_f(\bar{x}(t_f), t_f)}{\partial t} - \bar{\mu}_f^T \frac{\partial g_f(\bar{x}(t_f), t_f)}{\partial t} \quad (9)$$

$$\bar{p}(t_f) = \frac{\partial K_f(\bar{x}(t_f), t_f)}{\partial \bar{x}} + \frac{\partial g_f(\bar{x}(t_f), t_f)}{\partial \bar{x}} \bar{\mu}_f \quad (10)$$

To derive this estimator we will define the costs and the degrees of freedom. This will include three costs: one initial boundary cost, one final boundary cost, and a Lagrangian evaluated across the timespan of interest. We will limit the problem to timed fixed, free initial and final state optimization. Deriving an estimator through the Pontryagin Minimum Principle has been addressed before by Athans and Tse [17], but with a completely different cost function, framework, and results as compared to this study. We show the development of this estimator in the following section with a discussion of its properties.

III. OPTIMAL-CONTROL BASED ESTIMATOR

In this section we define the cost functions of the Optimal Control Based Estimator (OCBE), and the resulting time and measurement update equations. A discussion of the estimator's properties follows. We will not conclusively prove all of these properties, as we will focus more on the control analysis algorithms in the following section. A full development of the OCBE (including a nonlinear version) and proofs of it properties can be found in another study by the authors [7].

We seek an algorithm that infuses dynamics estimation with state estimation. To do this we infuse an optimal control process into a more traditional state estimation algorithm. Proceeding from our discussion of optimal control, we first define the cost function terms of interest. These include an a priori state deviation term (Eqn. 11), a measurement residual term (Eqn. 12), and control Lagrangian term (Eqn. 13).

$$K_{k-1} = \frac{1}{2} (\bar{x}_{k-1} - \hat{x}_{k-1})^T \bar{P}_{k-1}^{-1} (\bar{x}_{k-1} - \hat{x}_{k-1}) \quad (11)$$

$$K_k = \frac{1}{2} (\bar{Y}_k - h(t_k, \bar{x}_k))^T R_k^{-1} (\bar{Y}_k - h(t_k, \bar{x}_k)) \quad (12)$$

$$\mathcal{L}(\bar{x}(t), \bar{u}(t), t) = \frac{1}{2} \bar{u}(t)^T \bar{Q}^{-1} \bar{u}(t) \quad (13)$$

The a priori term incorporates previous information into the estimation process. In this notation, \bar{x}_{k-1} is the state we predict at time t_{k-1} , and \bar{P}_{k-1} is the corresponding covariance matrix. Unlike a Kalman filter, we do not propagate the a priori information to the measurement epoch. This decouples a priori state uncertainty and dynamic uncertainty in the estimation process so that we can account for each separately. We also leave the initial state free, which leads to state estimates at both the measurement epoch and the a priori epoch.

The measurement cost folds in information from measurements. In this notation, \bar{Y}_k is a vector of all measurements

taken at time t_k (no specific type is required), R_k is the covariance associated with those measurements, and $h(t, \bar{x})$ is a function that maps a state to its associated measurement (the observation-state relationship). This fully nonlinear term seeks to limit the measurement epoch state estimate from the measurement manifold conditioned on uncertainty in those measurements.

As defined, the a priori epoch and measurement epoch state estimates are independent. To connect them we incorporate an optimal control policy and enforce the system dynamics. We desire to minimize this control scheme (\bar{u}) conditioned on the scaled uncertainty in the dynamics (\bar{Q} , scaled by the time gap between the a priori and measurement epochs) because the control is an artificial process in the system (though it can represent mismodeled dynamics), so it should be on the level of uncertainty in the dynamics.

Using the initial and final adjoint transversality conditions (Eqns. 8 and 10) one can obtain an estimate for the initial and final adjoints in terms of the true initial and final states (Eqns. 14 and 15). We can also obtain an expression for the optimal control policy in terms of the adjoint (Eqn. 16).

$$\hat{p}_{k-1} = -\frac{\partial K_0}{\partial \bar{x}_{k-1}}^T = \bar{P}_{k-1}^{-1} (\bar{x}_{k-1} - \bar{x}_{k-1}) \quad (14)$$

$$\hat{p}_k = \frac{\partial K_f}{\partial \bar{x}_k}^T = -\frac{\partial h}{\partial \bar{x}_k}^T R_k^{-1} (\bar{y}_k - h(t_k, \bar{x}_k)) \quad (15)$$

$$\bar{u}(t) = -\bar{Q} \frac{\partial \bar{f}}{\partial u}^T \bar{p}(t) \quad (16)$$

Now we will linearize the system in order to obtain a linear estimator. We define a nominal ballistic trajectory ($\bar{u}(t) = 0 \forall t$) and the associated solution flow (Eqn. 17), which results in linearized initial and final adjoints as shown in Eqns. 18 and 19 (the δ 's in these and future equations refer to linearized values evaluated with respect to the nominal trajectory).

$$\bar{x}(t) = \phi_x(t; t_{k-1}, \bar{x}_{k-1}, \bar{p}_{k-1} = 0) \quad (17)$$

$$\bar{p}(t) = \phi_p(t; t_{k-1}, \bar{x}_{k-1}, \bar{p}_{k-1} = 0) = 0$$

$$\delta \hat{p}_{k-1} = \bar{P}_{k-1}^{-1} (\delta \bar{x}_{k-1} - \delta \bar{x}_{k-1}) \quad (18)$$

$$\delta \hat{p}_k = -\tilde{H}_k^T R_k^{-1} (\delta \bar{y}_k - \tilde{H}_k \delta \bar{x}_k) \quad (19)$$

After linearizing the system about a nominal trajectory we can describe motions in the vicinity through use of the State Transition Matrix (STM). The state motions are described in Eqn. 20, the adjoint motions are described in Eqn. 21, and the STM quadrants are defined in Eqn. 22. These equations combined with the linearized transversality conditions can be rearranged to solve for the states and adjoints at both epochs in terms of a priori state and measurement information. For notational convenience we will drop the time arguments in the STM for the remainder of this study, but it is implied

that the matrix is evaluated between the a priori epoch (t_{k-1}) and the measurement epoch (t_k).

$$\delta \hat{x}_k = \Phi_{xx}(t_k, t_{k-1}) \delta \hat{x}_{k-1} + \Phi_{xp}(t_k, t_{k-1}) \delta \hat{p}_{k-1} \quad (20)$$

$$\delta \hat{p}_k = \Phi_{px}(t_k, t_{k-1}) \delta \hat{x}_{k-1} + \Phi_{pp}(t_k, t_{k-1}) \delta \hat{p}_{k-1} \quad (21)$$

$$\Phi(t_k, t_{k-1}) = \begin{bmatrix} \Phi_{xx}(t_k, t_{k-1}) & \Phi_{xp}(t_k, t_{k-1}) \\ \Phi_{px}(t_k, t_{k-1}) & \Phi_{pp}(t_k, t_{k-1}) \end{bmatrix} \quad (22)$$

$$= \begin{bmatrix} \frac{\phi_x(t_k)}{\frac{\partial \bar{x}_{k-1}}{\partial \bar{x}_{k-1}}} & \frac{\phi_x(t_k)}{\frac{\partial \bar{p}_{k-1}}{\partial \bar{p}_{k-1}}} \\ \frac{\phi_p(t_k)}{\frac{\partial \bar{x}_{k-1}}{\partial \bar{x}_{k-1}}} & \frac{\phi_p(t_k)}{\frac{\partial \bar{p}_{k-1}}{\partial \bar{p}_{k-1}}} \end{bmatrix}$$

Before combining these four equations, it is important to note some STM properties. Using the results of Lubey and Scheeres [6], we find the relations between the portions of the STM as summarized in Eqn. 23. These result from the symplectic and ballistic properties of the system.

$$\begin{aligned} \Phi_{px} &= 0 \\ \Phi_{pp} \Phi_{xx}^T &= I \\ \Phi_{xp} \Phi_{xx}^T &= (\Phi_{xp} \Phi_{xx}^T)^T \end{aligned} \quad (23)$$

With the transversality conditions, the linearized motion equations, and the STM properties we obtain the measurement update equations for the OCBE as shown in Eqns. 24 - 27.

$$\delta \hat{x}_{k-1} = \delta \bar{x}_{k-1} + \Phi_{pp}^T \bar{P}_k \Psi_k (\delta \bar{y}_k - \tilde{H}_k \delta \bar{x}_k) \quad (24)$$

$$\delta \hat{x}_k = \delta \bar{x}_k + L_k (\delta \bar{y}_k - \tilde{H}_k \delta \bar{x}_k) \quad (25)$$

$$\delta \hat{p}_{k-1} = -\Phi_{xx}^T \Psi_k (\delta \bar{y}_k - \tilde{H}_k \delta \bar{x}_k) \quad (26)$$

$$\delta \hat{p}_k = -\Psi_k (\delta \bar{y}_k - \tilde{H}_k \delta \bar{x}_k) \quad (27)$$

Definitions of terms used in the above equations are provided in Eqns. 28 - 31. The first three equations are the time update equations for this estimator, and the fourth is the gain matrix used to weight the innovations against the a priori knowledge in Eqn. 25.

$$\delta \bar{x}_k = \Phi_{xx} \delta \bar{x}_{k-1} \quad (28)$$

$$\bar{P}_k = \Phi_{xx} P_{k-1} \Phi_{xx}^T \quad (29)$$

$$\mathcal{P}_k = \bar{P}_k - (\Phi_{xp} \Phi_{xx}^T) \quad (30)$$

$$L_k = \mathcal{P}_k \tilde{H}_k^T (R_k + \tilde{H}_k \mathcal{P}_k \tilde{H}_k^T)^{-1} = \mathcal{P}_k \Psi_k \quad (31)$$

Finally, it is necessary to provide some level of uncertainty in our state estimates. Equations 32 and 33 are the covariance of the state estimates at the a priori and measurement epoch, respectively.

$$\hat{P}_{k-1} = \bar{P}_{k-1} - \bar{P}_{k-1} \Phi_{xx}^T \tilde{H}_k^T (R_k + \tilde{H}_k \mathcal{P}_k \tilde{H}_k^T)^{-1} \tilde{H}_k \Phi_{xx} \bar{P}_{k-1} \quad (32)$$

$$\hat{P}_k = (I - L_k \tilde{H}_k) \mathcal{P}_k (I - L_k \tilde{H}_k)^T + L_k R_k L_k^T \quad (33)$$

Looking at all of these equations, we can make clear comparisons to the Kalman filter. It can actually be shown that this estimator is a generalization of the Kalman filter, and in this linear case the two algorithms yield the same state estimate and covariance (Eqns. 25 and 33). This results from demonstrating that the propagated covariance matrix with dynamic noise (Eqn. 30) is identical to propagating the covariance with continuous process noise as shown in Eqn. 34. Additionally, we can show that the a priori epoch state estimate and covariance are equivalent to a one step smoother (Eqns. 35 and 36 - notation from Tapley, Schutz, and Born [18]). In this notation subscripts refer to the time epoch at which the state and covariance are evaluated and the superscript in parentheses refers to the time epoch through which observations are considered (e.g. $\delta\hat{x}_{k-1}^{(k)}$ refers to the linearized best estimate of the state at t_{k-1} conditioned on all measurements through t_k). With these results we find that not only does the OCBE act as a Kalman filter, it also automatically includes dynamic noise equivalent to continuous process noise and smooths the estimate at the previous epoch.

$$\begin{aligned}\mathcal{P}_k &= \bar{\mathcal{P}}_k - (\Phi_{xp}\Phi_{xx}^T) \\ &= \Phi_{xx}(t_k, t_{k-1})\mathcal{P}_{k-1}\Phi_{xx}^T(t_k, t_{k-1})^T \\ &\quad + \int_{t_0}^t \Phi_{xx}(t, \tau) \frac{\partial \tilde{f}}{\partial \tilde{u}} \tilde{Q} \frac{\partial \tilde{f}^T}{\partial \tilde{u}} \Phi_{xx}^T(t, \tau) d\tau\end{aligned}\quad (34)$$

$$\begin{aligned}\delta\hat{x}_{k-1} &= \delta\bar{x}_{k-1} + (\bar{\mathcal{P}}_{k-1}\Phi_{xx}^T\mathcal{P}_k^{-1})[\delta\hat{x}_k - \Phi_{xx}\delta\bar{x}_{k-1}] \\ &= \delta\bar{x}_{k-1}^{(k-1)} + S_{k-1}[\delta\hat{x}_k^{(k)} - \Phi_{xx}\delta\hat{x}_{k-1}^{(k-1)}] \\ &= \delta\hat{x}_{k-1}^{(k)}\end{aligned}\quad (35)$$

$$S_{k-1} = \mathcal{P}_{k-1}^{(k-1)}\Phi_{xx}^T(\mathcal{P}_k^{(k-1)})^{-1}\quad (36)$$

One of the most important pieces of information that comes out of this estimator is the control policy (Eqn. 37). From this control policy we can identify mismodeled natural dynamics as well as detect maneuvers and reconstruct them. In the next section we will explore two methods for extracting information from this control policy.

$$\delta\tilde{u}(t) = -\tilde{Q} \frac{\partial \tilde{f}^T}{\partial u} \Phi_{pp}(t, t_{k-1}) \delta\hat{p}_{k-1}\quad (37)$$

IV. CONTROL POLICY ANALYSIS

The control policies that come out of the OCBE contain information relating to the mismodeled dynamics in the system. In this section we demonstrate two methods to extract that information. The first method focuses on determining whether mismodeled dynamics are present or not. The second method attempts to attribute those control accelerations to a known perturbation. Aside from these two methods, the control profiles by themselves have meaning. They are a model for how the system moves from one state to the next. Consistent biasing generally indicates mismodeled dynamics, and unmodeled maneuvers will stick out as one-time events.

A. Maneuver Detection

This maneuver detection method is based on control distance metrics as defined by Holzinger, Scheeres, and Alfried [4]. We use a weighted metric (Eqn. 38) since this was used in the estimator derivation. Having linearized about a ballistic trajectory, the full control profile is defined by Eqn. 37. Subbing this into the distance metric (with the results of Eqn. 26) we obtain the distance metric as a function of the measurements and a priori information (Eqn. 39) with a definition made in Eqn. 40.

$$D_C = \int_{t_{k-1}}^{t_k} \frac{1}{2} \tilde{u}(\tau)^T \tilde{Q}^{-1} \tilde{u}(\tau) d\tau\quad (38)$$

$$D_C = (\delta\tilde{y}_k - \tilde{H}_k \delta\bar{x}_k)^T \Psi_k^T \Phi_{xx} \Pi_k \Phi_{xx}^T \Psi_k (\delta\tilde{y}_k - \tilde{H}_k \delta\bar{x}_k)\quad (39)$$

$$\Pi_k = \frac{1}{2} \left[\int_{t_{k-1}}^{t_k} \Phi_{pp}(\tau, t_{k-1})^T \frac{\partial \tilde{f}}{\partial u} \tilde{Q} \frac{\partial \tilde{f}^T}{\partial u} \Phi_{pp}(\tau, t_{k-1}) d\tau \right]\quad (40)$$

The innovations are assumed to be zero mean, considering without measurement information included it would be a mean zero random variable. With this assumption we obtain the following statistics on the distance metric (Eqns. 41 and 42). Using these statistics we can define a maneuver threshold at a strong positive value relative to the distribution. Assuming the distribution is Gaussian (an assumption considering it should be skewed due to the positive definite nature of a control distance metric) we can define the threshold at a particular z-score (e.g. $z = 1.96$ for a 95% confidence level). When the distance metric calculated from Eqn. 39 exceeds this threshold, we conclude that some unknown acceleration is present in the system. We can then proceed with analyzing the associated control profile for information about this unknown acceleration.

$$\mu_{D_C} = \text{Trace}[\Pi_k (R_k + \tilde{H}_k \mathcal{P}_k \tilde{H}_k^T)]\quad (41)$$

$$\sigma_{D_C}^2 = 2(\text{Trace}[\Pi_k (R_k + \tilde{H}_k \mathcal{P}_k \tilde{H}_k^T) \Pi_k (R_k + \tilde{H}_k \mathcal{P}_k \tilde{H}_k^T)])\quad (42)$$

The level of dynamic uncertainty (\tilde{Q}) largely controls whether a maneuver is detected. When maneuvers are consistently detected this generally implies the dynamic uncertainty does not adequately capture the true level of uncertainty (it should be raised). Adjusting this uncertainty matrix in this manner can reveal the true level of dynamic uncertainty in the system.

When a series of measurements has many maneuvers detected we can generally conclude that there is continuous mismodeling in the system. On the other hand, one maneuver detected in a series of measurements is more indicative of an unmodeled maneuver. This designation is important to make when approaching reconstruction of the unknown dynamics. The following algorithm offers a method for estimating consistent dynamics mismodeling when a model for the acceleration is available.

B. Natural Dynamics Estimation

When a consistent dynamics mismatching has been identified one method for recovering the underlying dynamics is by assuming that the control policy is a good model for those dynamics, and selecting the scaling parameter for the perturbation such that it minimizes the the cost function in Eqn. 43. This cost function attempts to allocate the control policy to linearly mismatched perturbations. The perturbations must be able to be written in the form of $\Delta\tilde{C}$ where the parameters are contained in $\Delta\tilde{C}$.

$$\mathcal{J}_{ND} = \frac{1}{2} \int_{t_{k-1}}^{t_k} (\tilde{u}(\tau) - \tilde{A}(\tau, \tilde{x})\Delta\tilde{C})^T (\tilde{u}(\tau) - \tilde{A}(\tau, \tilde{x})\Delta\tilde{C}) d\tau \quad (43)$$

Minimizing this cost function and expanding the control in terms of boundary state variations ($\delta\tilde{z} = [\delta\tilde{x}_{k-1}^T \delta\tilde{x}_k^T]^T$), we obtain Eqn. 44 with definitions made in Eqns. 45 - 49. The associated covariance with this estimate is found in Eqn. 50. In this expression P_z contains the covariances of the state estimates at each epoch on the diagonal. The nominal trajectory is ballistic so the associated control policy is zero ($\tilde{u}^*(t) = \tilde{0}$), which means the first term is zero. The $\delta\tilde{z}$ term and its covariance is obtained through the OCBE. For highly nonlinear systems this process should be iterated several times to obtain a reliable parameter estimate. This requires obtaining a control profile, estimating the dynamics, updating the dynamical model, obtaining a new control profile, and repeating until convergence is attained. This is more thoroughly described in Lubey and Scheeres [10].

$$\Delta\tilde{C} = M(t_k, t_{k-1}) \left[\int_{t_{k-1}}^{t_k} \tilde{A}(\tau, \tilde{x})^T \tilde{u}^*(\tau) d\tau - V(t_k, t_{k-1}) \delta\tilde{z} \right] \quad (44)$$

$$M(t_k, t_{k-1}) = \left(\int_{t_{k-1}}^{t_k} \tilde{A}(\tau, \tilde{x})^T \tilde{A}(\tau, \tilde{x}) d\tau \right)^{-1} \quad (45)$$

$$V(t_k, t_{k-1}) = \int_{t_{k-1}}^{t_k} \tilde{A}(\tau, \tilde{x})^T \tilde{Q} \frac{\partial \tilde{f}^T}{\partial \tilde{u}} \Lambda(\tau, t_{k-1}) d\tau \quad (46)$$

$$\Lambda(t, t_0) = \begin{bmatrix} \Lambda_{k-1}(t, t_0) & \Lambda_k(t, t_0) \end{bmatrix} \quad (47)$$

$$\Lambda_{k-1}(t, t_0) = \Phi_{px}(t, t_0) - \Phi_{pp}(t, t_0) \Phi_{xp}(t_f, t_0)^{-1} \Phi_{xx}(t_f, t_0) \quad (48)$$

$$\Lambda_k(t, t_0) = \Phi_{pp}(t, t_0) \Phi_{xp}(t_f, t_0)^{-1} \quad (49)$$

$$P_{\Delta C} = M(t_k, t_{k-1}) V(t_k, t_{k-1}) P_z V(t_k, t_{k-1})^T M(t_k, t_{k-1})^T \quad (50)$$

This algorithm is made more powerful in a batch formulation. The equations for combining the parameter estimates into a single estimate are given below.

$$\Delta\tilde{C} = \left(\sum_{i=1}^N P_{\Delta C_i}^{-1} \right)^{-1} \left(\sum_{i=1}^N P_{\Delta C_i}^{-1} \Delta\tilde{C}_i \right) \quad (51)$$

$$P_{\Delta C} = \left(\sum_{i=1}^N P_{\Delta C_i}^{-1} \right)^{-1} \quad (52)$$

This algorithm is made general for any system, but its effectiveness requires that a least-squares optimal control

policy accurately replicates the dynamics it replaces. It has been shown by the authors that atmospheric drag and solar radiation pressure in an orbital environment are two perturbations that are well replicated by these control policies. The following numerical simulation demonstrates this algorithm (state estimation, control estimation, maneuver detection, and natural dynamics estimation) in such a scenario.

V. NUMERICAL SIMULATION

In this simulation we track an object in Low Earth Orbit (LEO) with range and range rate measurements taken once each hour for 150 continuous hours. The measurements have 0.1 m and 1 mm/s error, respectively. The drag parameter we start with is flawed with a 12.5% overestimate, which makes this a mismatched dynamics estimation problem. The modeled dynamics include two body gravity, J2 (oblateness) gravity effects, atmospheric drag, and solar radiation pressure. The latter two perturbations are subject to mismatching since they are the only two object-dependent forces. Relevant dynamics parameters and the initial conditions are given in Table I.

TABLE I
TRUE SPACECRAFT PARAMETERS AND INITIAL CONDITIONS FOR TEST CASE

Parameter	Symbol	Value	Units
Mass	m	970	kg
Drag Parameter	B	0.0062	m ² /kg
SRP Parameter	P	0.0031	m ² /kg
Initial Semimajor Axis	a_0	7172.498	km
Initial Eccentricity	e_0	0.001	-
Initial Inclination	i_0	98.620	deg
Initial Right Asc. of the Asc. Node	Ω_0	253.734	deg
Initial Argument of Perigee	ω_0	77.203	deg
Initial Mean Anomaly	M_0	59.490	deg

As discussed when developing the maneuver detection algorithm, detecting maneuvers is heavily dependent on the level of dynamic uncertainty set in the algorithm. When we undershoot the true level we end up detecting maneuvers at almost every epoch. When we overshoot the true level, we artificially suppress maneuvers. When we use the true level of dynamic uncertainty the maneuver detection results are distributed appropriately according to the analytical statistical metrics. Maneuver detection results for two levels of uncertainty are provided in Fig. 2. From these results we see that maneuvers are routinely detected for the 1E-09 m/s² level of uncertainty. When we raise that level to 1E-08 m/s² the maneuver detection results are distributed appropriately. This indicated that the ideal level of dynamic uncertainty is 1E-08 m/s², which corresponds to a 12.5% overestimate in atmospheric drag for this situation. This demonstrates how this algorithm may be used to identify a consistent mismatching as well as get an order of magnitude estimate for the level of that uncertainty.

The tracking performance of the OCBE with various levels of dynamic uncertainty is shown in the true state deviations of Fig. 2. In these results we confirm the results from the maneuver detection analysis. Specifically, that a dynamic

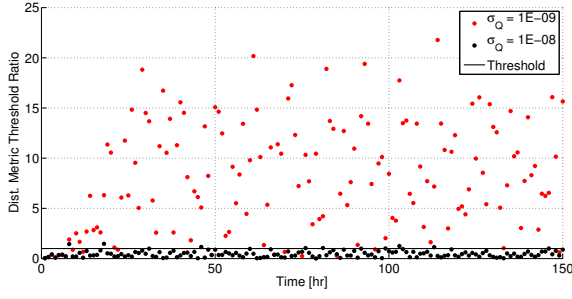


Fig. 1. Maneuver detection results for dynamic uncertainty levels of $\sigma_Q = 1e-09$ (red) and $1e-08$ (black) m/s^2 .

uncertainty of $1E-08 m/s^2$ exists in the system. We see degraded performance for all other levels of uncertainty (higher and lower). We also see the equivalence with the process-noise free Kalman filter when a dynamic uncertainty of zero is used. This numerically backs up the analytical result that the OCBE is a generalization of the Kalman filter.

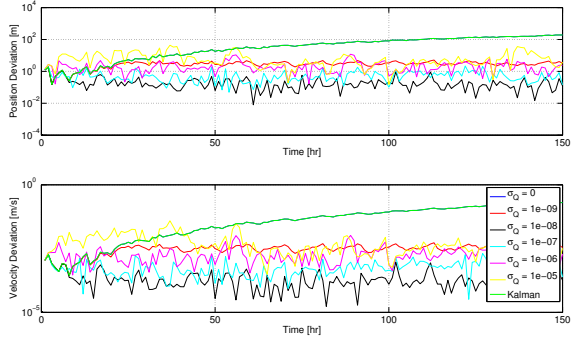


Fig. 2. Position deviations from truth. σ_Q is the level of uncertainty in the dynamics in m/s^2 and KF is the Kalman Filter output.

Having identified a consistent mismodeling, we proceed with applying the natural dynamics estimation method. The results from one pass of the data are shown in Fig. 3. In these results the spread in SRP estimates is far greater than drag estimates because drag is the dominant perturbation. This makes the drag parameter less sensitive to changes in the control. The SRP estimates are not too reliable with this huge spread so we will neglect them for this analysis. For drag estimation, with each pass through the data we get closer to the true value. After 4 iterations we obtain approximately 1% error in the drag parameter from the original 12.5% error. This large reduction in error demonstrates the accuracy of this algorithm in using information from these control estimates to estimate natural dynamics.

This example clearly demonstrates the use of all aspects of this algorithm: state estimation, control estimation, maneuver detection, and natural dynamics estimation. With an overestimate in drag, the OCBE maintained tracking, the maneuver detection algorithm identified the presence of mismodeled dynamics and its order of magnitude, and the natural dynamics estimation method accurately estimated the

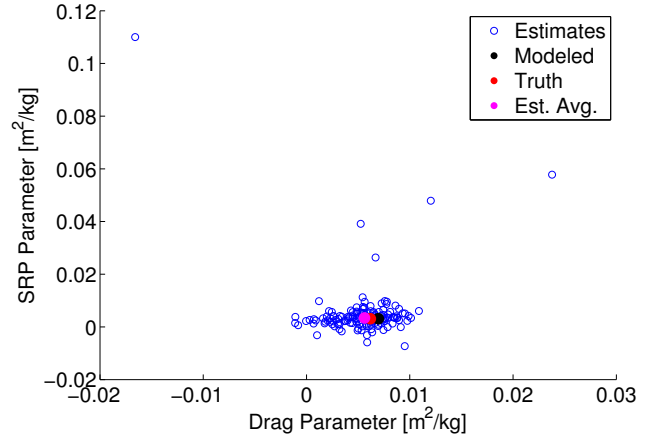


Fig. 3. Atmospheric drag and SRP parameter estimates for each observation epoch. The initial modeled value (black), truth (red), and the batch estimate (purple) are indicated.

mismodeling. Through this we have shown the ability of this algorithm to deal with a dynamically mismodeled system as well as extract information about that mismodeling.

VI. CONCLUSIONS

In this paper, we have outlined how control can be included in the estimation process to create a robust estimator that is a generalization of the Kalman filter. This estimator not only provides equivalent state and state uncertainty estimates to the Kalman filter, it also has automatic dynamic noise propagation, smoothing, and control estimation properties. Those control estimates can then be used to understand dynamic mismodeling in the system. This includes using the control to detect mismodeled dynamics as well as estimate natural dynamics it may be replicating. The algorithms written are intended for any generic system. The natural dynamics estimation algorithm has certain requirements to be effective, but all other aspects are applicable to any system that is linearizable. An example application of tracking an object in orbit with an erroneous drag model demonstrated the use of this algorithm in estimating in dynamically mismodeled systems.

The problem of estimating in a system with mismodeled dynamics is a common one that spans all fields of science and engineering. The algorithm developed here is a compact treatment of this problem that accomplishes what classical estimators do, and adds much more with the addition of information from estimated control policies.

ACKNOWLEDGMENT

This work was supported by a NASA Office of the Chief Technologists Space Technology Research Fellowship.

REFERENCES

- [1] Bar-Shalom, Y. & Birmiwal, K., *Variable Dimension Filter for Maneuvering Target Tracking*, Aerospace and Electronic Systems, Vol. 18, No. 5, pp. 621-629, 1982.
- [2] Chan, Y.T., Hu, A.G.C., & Plant, J.B., *A Kalman Filter Based Tracking Scheme with Input Estimation*, Aerospace and Electronic Systems, Vol. 15, No. 2, pp. 237-244, 1979.

- [3] Patera, R.P., *Space Event Detection Method*, Journal of Spacecraft and Rockets, Vol. 45, No. 3, 2008.
- [4] Holzinger, M.J., Scheeres, D.J., & Alfried, K.T., *Object correlation, maneuver detection, and characterization using control distance metrics*, Journal of Guidance, Control, and Dynamics, In Press 2011.
- [5] Singh N., Horwood J.T., & Poore A.B., *Space Object Maneuver Detection Via a Joint Optimal Control and Multiple Hypothesis Tracking Approach*, AAS 12-159, In Press 2012.
- [6] Lubey, D.P. & Scheeres, D.J., *Combined Optimal Control and State Estimation for the Purposes of Maneuver Detection and Reconstruction*, Proceedings of the 2014 American Control Conference, Portland, OR, 2014, in press.
- [7] Lubey, D.P. & Scheeres, D.J., *State and Dynamics Estimation with an Optimal Control Infused Estimator*, Proceedings of the 2014 Conference on Decision and Control, Los Angeles, CA, 2014, In press 2014.
- [8] Lubey, D.P. & Scheeres, D.J., *An Optimal Control Based Estimator for Maneuver Detection and Reconstruction*, Proceedings of the 2013 AAS/AIAA Astrodynamics Specialists Meeting, August 2013.
- [9] Lubey, D.P. & Scheeres, D.J., *An Optimal Control Based Estimator for Maneuver and Natural Dynamics Reconstruction*, Proceedings of the 2013 Advanced Maui Optical and Space Surveillance Technologies Conference, September 2013.
- [10] Lubey, D.P. & Scheeres, D.J., *Identifying and Estimating Mismodeled Dynamics via Optimal Control Problem Distance Metrics*, Journal of Guidance, Control, and Dynamics, In Press 2014.
- [11] Lawden, D.F., *Optimal Trajectories for Space Navigation*, Butterworths Mathematical Texts, 1963.
- [12] Lawden, D.F., *Analytical Methods of Optimization*, Dover Publications Inc., 1975.
- [13] Marec, J.P., *Optimal Space Trajectories*, Elsevier Press, 1979.
- [14] Stengel, R.F., *Optimal Control and Estimation*, Dover Publications Inc., 1986.
- [15] Prussing, J.E. & Chiu, J.H., *Optimal Multiple-Impulse Time-Fixed Rendezvous Between Circular Orbits*, AIAA Journal, Vol. 9, No.1, Feb. 1986.
- [16] Prussing, J.E., *Optimal Two- and Three-Impulse Fixed-Time Rendezvous in the Vicinity of a Circular Orbit*, AIAA Journal, Vol. 8, No. 7, 1970, pp. 1221-1228.
- [17] Athans, M. & Tse, E., *A Direct Derivation of the Optimal Linear Filter Using the Maximum Principle*, IEEE Transactions on Automatic Control, Vol. AC-12, No. 6, December 1967.
- [18] Tapley, B.D., Schutz, B.E., & Born G.H., *Statistical Orbit Determination*, Elsevier Academic Press, 2004.